New Method of Lifetime Prediction for Brittle Fracture of Polyethylene

A. CHUDNOVSKY,* Y. SHULKIN, D. BARON, and K. P. LIN

Department of Civil Engineering and Materials (M/C246), University of Illinois at Chicago, Chicago, Illinois 60680

SYNOPSIS

A new method for predicting the time to brittle failure of polyethylenes is proposed. The method includes modeling slow crack growth in polyethylenes and the experimental determination of material parameters for the model. The model is based on the concept of the crack layer, i.e., a system consisting of the strongly interacting crack and process zone and the kinetic equations which govern the crack layer growth. The process zone in polyethylenes usually appears to be a thin strip of drawn material extending along the crack line. This permits a characterization of the crack layer by two parameters: the crack and process zone lengths. The two-parameter crack layer kinetic model allows description of slow crack growth as the discontinuous (stepwise) process which is commonly observed in the brittle fracture of polyethylenes. The model also predicts a relationship between time to failure and applied stress, identical to that established experimentally. The material parameters of the kinetic model can be determined by experiments on smooth specimens, i.e., are independent of slow crack growth and require relatively short-term observations. Thus, the combination of the material testing and the mathematical modeling of the crack layer evolution is proposed as a method for lifetime prediction in the brittle fracture of polyethylenes. © 1995 John Wiley & Sons, Inc.

1. INTRODUCTION

The failure of polyethylene (PE) typically occurs as a result of either a shear rupture or a sudden onset of instability in a previously slowly growing crack. In both cases the time to failure depends greatly on temperature. Extensive data regarding the effect of temperature upon the relation between the lifetime and hoop stress for internally pressurized high-density PE pipes was reported by Williams.[1] Brown with co-workers[2-6] conducted experiments on single-edge notched tensile specimens and investigated at various temperatures the time to failure as a function of such variables as applied stress, specimen geometry, molecular weight distribution, and branch density. Analysis of the observations shows that at room temperature and relatively low-stress PEs may serve for decades. For example, the lifetime expectancy of PE pipes for natural gas distribution is about 50 years or more. An accelerated test for lifetime in long-term fracture processes is of a great importance for the evaluation of new PEs for engineering applications.

It was demonstrated by Brown et al.[5,6] for two kinds of polyethylene that a certain treatment of the experimental results obtained in short-term fracture tests (at high temperatures) under creep conditions allows a reasonable estimation of the long-term lifetime at room temperature. A formally different, but essentially equivalent, way of predicting the time to failure under creep was developed and presented as the universal procedure for PE piping materials by Popelar with co-workers.[7,8] According to these methods, in order to find the stress dependence of the time to failure at a low temperature, it is necessary to know the relationship between lifetime and stress at a high temperature, and either to recalculate the data or to make shifts in the stress and time axes following a simple recipe. In fact, the mentioned empirical approaches to lifetime prediction are extrapolations of data obtained in the range of variables where the phenomenon is

* To whom correspondence should be addressed.

Journal of Applied Polymer Science, Vol. 56, 1465–1478 (1995)
 CCC 0021-8995/95/111465-14

available for observation, to the range where direct measurements are unrealistic. Another empirical method to rank PEs, as well as to predict the lifetime in long-term creep processes was proposed by Moet with co-workers.[9] The method is based on the interpretation of creep as the limiting case of fatigue, when the ratio of the minimum to maximum stress approaches one.

To our knowledge, Kostrov et al.[10] were the first to consider a crack with a cohesive zone in a viscoelastic material. Later, theories of crack growth in viscoelastic media were advanced by many authors. The most detailed analysis of the problem was presented by Schapery[11] (see also references contained therein). Theory[11] is based on the following assumptions: (1) the stress field in the vicinity of the crack tip agrees with the Barenblatt cohesive zone model; (2) the classical correspondence principle for viscoelastic media is valid for the case of a moving crack; and (3) the crack grows, if and when the work done by the stress on the total elastic plus viscoelastic displacement at the root of the cohesive zone, reaches the value of specific fracture energy. The latter is considered to be a material constant. The viscoelastic model[11] predicts a smooth crack propagation under the creep condition, i.e., the crack growth rate monotonically increases with time. However, as has been observed for many polymers and for PEs specifically,[12,13] the process of slow crack growth under both creep and fatigue conditions proceeds in a discontinuous (stepwise) manner, i.e., the crack propagates via a succession of alternating advances and arrests. The stress dependence of lifetime at fixed temperature established in Ref. 11 is similar to the dependence commonly observed in experiments with polymers, and can be approximately expressed as a power law. However, the theoretical range of the exponent values differs appreciably from the experimental range reported for PEs.[2-6]

A new method of lifetime prediction for PEs under creep, which is presented in this paper, is based on the crack layer concept introduced by Chudnovsky[14] and developed by him with coworkers.[15-20] The crack layer (CL) is a system consisting of the closely coupled crack and process zone (PZ). The CL is characterized by the crack and PZ lengths and is therefore a system of two degrees of freedom. This results in the existence of various scenarios for the fracture process and more realistic modeling of slow crack growth behavior in PEs.

In this work, the previously proposed empirical relations between time to failure of PEs, under creep at various temperatures and applied stress, are presented and examined (Section 2). Then, a brief review of the CL kinetic model and its application for brittle fracture of PEs under creep conditions is presented (Section 3). The predictive power of the model is examined by comparing the theoretical time–stress–temperature relation with that obtained experimentally for a medium-density PE (Section 4). Finally, a new procedure for lifetime prediction that consists of the experimental determination of the material parameters and the numerical simulation of the CL growth is detailed (Section 5).

2. EMPIRICAL METHODS FOR LIFETIME PREDICTION

Comprehensive investigations of various PEs[1,5,6] has revealed the dependence of time to failure, t_f, on stress σ and temperature T schematically depicted in Figure 1 (T signifies temperature in degrees Kelvin). Fracture in the ductile mode occurs as a result of macroscopic shear rupture, and the time to failure in this process is mainly determined by the rate of viscoelastic deformation. The brittle mode of failure is associated with slow growth of a crack induced by a preexisting defect. The lifetime in this case is the time during which the crack initiates and slowly propagates, up to the ultimate instability leading to catastrophic failure. Within both modes of failure, ductile and brittle, the time–stress relation at a fixed temperature can be approximately expressed in the form

$$\log t_f = A - \alpha \log \sigma \tag{2.1}$$

where in Ref. 1 σ is the hoop stress in an internally pressurized pipe, and in Refs. 5 and 6 σ is the tensile stress applied to a single-edge notched (SEN) spec-

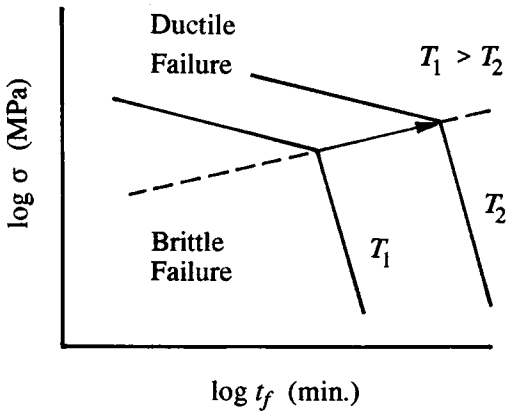

Figure 1 Schematic representation of experimental time–stress relations.

imen. In Eq. (2.1) "log" means the decimal logarithm, and the symbols t_f and σ represent dimensionless quantities, corresponding to the time to failure in minutes and stress in MPa, respectively. The first term, A, in the right-hand side of relation (2.1) is a function of temperature T, while values of coefficient α for ductile and brittle modes seldom, but sometimes, depend on temperature. For example, coefficient α in the case of the PE studied in Ref. 6 can be considered as temperature independent, but for another PE,[5] within the brittle mode α changes noticeably; increasing from 3.0 to 4.8, when the temperature increases from 42 to 80°C. As seen from Figure 1, the values of coefficient α for ductile and brittle modes differ greatly (about 10 or even 15 times according to Refs. 5 and 6, respectively). It should be noted that as shown in Refs. 5 and 6, there is a ductile–brittle transition zone, which has been reduced to a single point in Figure 1. The stress corresponding to the intersection of the two branches, ductile and brittle in Figure 1, is called the critical stress and denoted by σ_c. As can be seen from Figure 1, the critical stress is a decreasing function of temperature.

If coefficient α is independent of temperature, the ductile and brittle branches in Figure 1 form two sets of parallel lines. Lines for different temperatures can now be combined into one line by appropriate shifts. In order to encompass both the ductile and brittle branches, the shifts have to be directed along the arrow shown in Figure 1, i.e., the shifts contain two components, horizontal and vertical. The horizontal component is determined by the Arrhenius equation, according to which characteristic times t_1 and t_2 of the process for temperatures T_1 and T_2, respectively, are connected:

$$\frac{t_2}{t_1} = \exp \frac{Q}{R}\left(\frac{1}{T_2} - \frac{1}{T_1}\right)$$

where Q is the so-called activation energy (in J/mol) of the process, and R is the universal gas constant (R = 8.314 J/K mol). According to the above equation, the horizontal shift due to temperature variation from T_1 to T_2 is written in the form

$$\Delta h = 0.43 \frac{Q}{R}\left(\frac{1}{T_2} - \frac{1}{T_1}\right) \tag{2.2}$$

where the numerical factor is the value of log e. The vertical shift is expressed in terms of the temperature dependence of the critical stress σ_c; certain considerations regarding the causes for this shift can be found in Refs. 7 and 8. According to Ref. 5, for temperatures higher than 70°C, log σ_c is a linear function of inverse temperature T^{-1}. Let c be the coefficient of T^{-1} in this function. Then, the vertical shift

$$\Delta v = \log \frac{\sigma_c(T_2)}{\sigma_c(T_1)}$$

can be represented as follows:

$$\Delta v = c\left(\frac{1}{T_2} - \frac{1}{T_1}\right) \tag{2.3}$$

According to Ref. 5, $c \approx 0.42 \times 10^3$ K. If one assumes that shifts (2.2) and (2.3) are valid within the temperature range of interest (from 24 to 80°C, for example), then the lifetime at a low temperature T_2 (particularly, at room temperature) can be estimated on the basis of knowledge of the time–stress relation (2.1) for a high temperature T_1:

$$\log t_f(T_2) = \log t_f(T_1) + 0.43 \frac{Q}{R}\left(\frac{1}{T_2} - \frac{1}{T_1}\right) + c\left(\frac{1}{T_2} - \frac{1}{T_1}\right)$$

Shifts (2.2) and (2.3) were essentially employed by Lu and Brown for two kinds of PE.[5,6] This allowed them to reduce the time–stress relations at different temperatures to a single one for room temperature (24°C) and obtain, as a result, a master curve of "log t_f vs. log $\hat{\sigma}$" ($\hat{\sigma}$ is the applied stress σ, normalized by critical stress σ_c).

Popelar and co-workers[7,8] proposed different horizontal and vertical shifts:

$$\Delta h = 0.43 \times 0.1090(T_1 - T_2) \tag{2.4}$$

$$\Delta v = 0.43 \times 0.0116(T_1 - T_2) \tag{2.5}$$

as universal, for the medium-density and high-density PEs that are commonly used in natural gas distribution piping. To determine how shifts (2.2) and (2.3) are related to shifts (2.4) and (2.5), note first that within the temperature range of 293–353 K (20–80°C), the approximate equality (with a maximum error of about 15%) exists:

$$\frac{1}{T_2} - \frac{1}{T_1} \approx 0.96 \times 10^{-5}(T_1 - T_2)$$

Then, as follows from equating Eqs. (2.2) and (2.4), the required value of Q (activation energy) in Eq. (2.4) is $\approx$ 94 kJ/mol (with the same maximum error). For the PEs discussed, the value of the activation energy for fracture processes is usually reported around 100 kJ/mol. Equating Eqs. (2.3) and (2.5) shows that the vertical shift proposed in Refs. 7 and 8 corresponds to the following value of coefficient c:

$$c \approx 0.52 \times 10^3 \text{ K}$$

Recall that as indicated above, the value of this coefficient for the material studied in Ref. 5 should be taken as 0.42×10^3 K.

Therefore, shifts (2.4) and (2.5) are essentially the same as shifts (2.2) and (2.3). Quantitatively, they should be considered as certain, empirically evaluated quantities, that reflect on average the relationship between time to failure and stress, at various temperatures. In spite of a good average agreement, in some cases the lifetime predicted by the empirical method[7,8] may noticeably deviate from that measured directly. For example, for the PE examined in Ref. 6, the relation between lifetime and stress was experimentally found either at 80 or at 24°C. In this case coefficient α from Eq. (2.1) did not depend on temperature. The prediction of brittle failure at 24°C by means of shifts (2.4) and (2.5), from the data obtained at 80°C, forecasts a lifetime 10 times greater than the actual lifetime (see Appendix A). For another PE,[5] the lowest temperature under which the measurements of the lifetime were conducted was 42°C and the highest was 80°C. As noted above, according to direct observations, coefficient α within the brittle mode is temperature dependent. In this case the transition from 80 to 42°C, with shifts (2.4) and (2.5), at low stresses overestimates the lifetime more than 10 times (see Appendix B). The empirical methods[5,6] and Refs. 7 and 8 rely substantially on the concept of the critical stress σ_c of ductile–brittle transition, and on the temperature dependence of this stress. Above, σ_c has been defined as the ordinate of the boundary point between the ductile and brittle regions, on the graph of Figure 1. However, there is no reason to consider this quantity as a material property that is independent of specimen geometry and loading conditions. In addition, since the measurements in long-term observations have a large scatter, the critical stress can only be determined statistically. The most important drawback of the method of temperature shifts for the stress and time axes is common to all empirical approaches: the limitation of the method's applicability, and the error resulting from its application, are *a priori* unknown.

The following considerations are concerned with brittle fracture. From a practical point of view, it is the most important case, since the PEs in engineering applications serve mostly under relatively low stresses and undergo the brittle mode of failure. The method of lifetime prediction presented below is based on the mathematical modeling of slow crack growth in PEs under creep conditions and describes in a natural way a connection between short-term and long-term failure processes. An important distinction of the new method is that it explicitly accounts for material properties, specimen geometry, and loading conditions.

3. MODEL OF CRACK GROWTH

In simple tension tests, most PEs exhibit cold drawing (necking) with constant drawing stress σ_{dr} and natural draw ratio λ_n. The cold drawing results in formation of a highly oriented material with properties different from the original one. For different PEs, the drawing stress at room temperature varies approximately from 15 to 25 MPa, and the natural draw ratio changes from 3 to 10.

In many engineering polymers, including PE, a slow growing crack is usually preceded by a PZ consisting of drawn material (Fig. 2). According to Ref. 14, the crack and PZ together form a CL. The simplified model of the crack layer developed in Refs. 15–17 is characterized by two parameters, the crack length l and the crack layer length L (Fig. 3). The bulk material surrounding the CL is the original material, while the PZ consists of the drawn material. This material can be treated as a collection of separate fibers[2–6] (see also Fig. 2) and can be modeled as a disconnected unidirectional continuum. As has been found by measurements,[21,22] the stresses acting between the bulk material and PZ are distributed uniformly along their boundary. Under the creep condition these stresses are controlled by the drawing process and can be assumed to be equal to the drawing stress, σ_{dr}.

The driving forces for the crack and PZ advances have been introduced in Refs. 14 and 15, in agreement with the general principle of irreversible thermodynamics:

$$X_{CR} = -\frac{\partial G}{\partial l} \quad X_{PZ} = -\frac{\partial G}{\partial L}$$

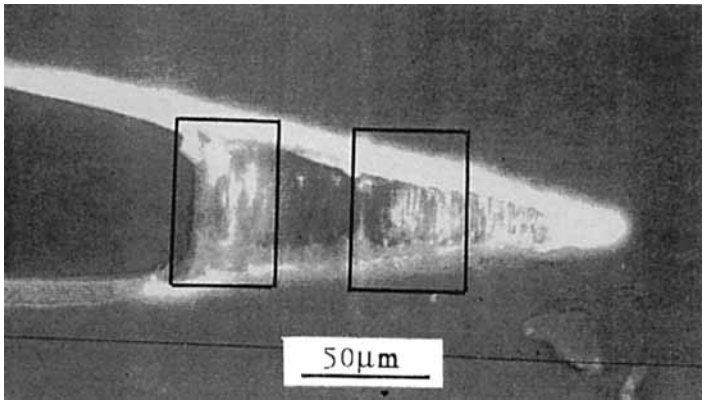

(a)

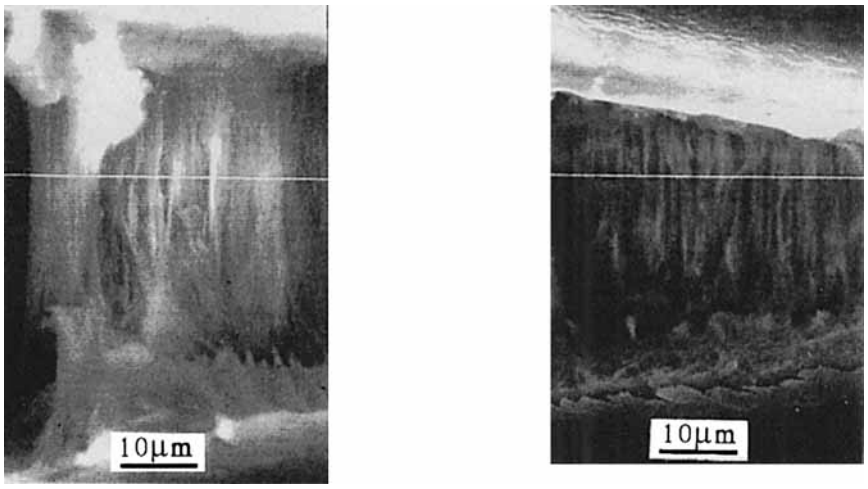

(b)

Figure 2 ESEM micrograph of the crack tip and the process zone developed under fatigue: (a) the general view, (b) fibrillated material within the process zone.

where G is the Gibbs potential of the particular system. Since no healing process exists within any presently known material, the crack and PZ sizes cannot decrease. Therefore, it is assumed that $X_{CR} = 0$ and $X_{PZ} = 0$ if the corresponding derivatives of G are not positive. According to Refs. 15 and 18, the process of CL propagation is governed by equations

$$\frac{dl}{dt} = k_1 X_{CR} \quad \frac{dL}{dt} = k_2 X_{PZ} \tag{3.1}$$

with initial conditions

$$l = l_0 \quad L = L_0 \quad \text{at } t = 0$$

Below, only mode 1 loading is examined. The driving force for the crack advance is derived in the form[15,18,19]

$$X_{CR} = J_1 - 2\gamma \tag{3.2}$$

with

$$J_1 = \sigma_{dr}[\delta_\infty + (1 + \tilde{\gamma})\delta_\infty]$$

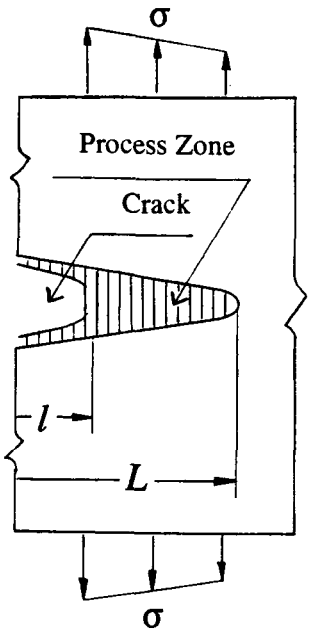

Figure 3 Schematic presentation of crack layer in PEs.

or

$$X_{CR} = 0 \tag{3.2'}$$

depending on whether the derivative of G with respect to l is positive or not. Above, δ_∞ and δ_{dr} represent the elastic crack opening displacements (CODs) due to remote stress σ, and traction σ_{dr} acting along the PZ boundary of the problem depicted in Figure 4. Since the PZ has the shape of a thin strip, the cut-out in Fig. 4 (a) can be modeled by the slit in Fig. 4 (b). Moreover,

$$\tilde{\gamma} = \frac{\gamma_{dr}}{\sigma_{dr}(\lambda - 1)}$$

is the specific energy of drawing, γ_{dr}, normalized by the mechanical work of drawing, $\sigma_{dr}(\lambda - 1)$. Finally, γ signifies the specific energy (per unit area) required for rupture of the PZ fibers and membranes. Sometimes for convenience, J_1 and 2γ in Eq. (3.2) are, respectively, referred to as the active part of the driving force X_{CR} and the resistance to crack extension.

Fibers within the PZ experience viscoelastic deformation, and as a result the specific fracture energy, γ, of the PZ material decreases. The law of γ evolution with time is derived below from the following considerations. Let ε_e and ε_v be the elastic and viscoelastic deformation of the drawn material, so that the total strain is written in the form

$$\varepsilon(t) = \varepsilon_e + \varepsilon_v(t)$$

At the initial instant, the energy γ_0 required for fiber rupture, is equal to the work done by the drawing stress σ_{dr} on a certain critical viscoelastic strain ε_{vc}:

$$\gamma_0 = \sigma_{dr}\varepsilon_{vc}$$

For the current moment, the energy γ can be defined as follows:

$$\gamma(t) = \gamma_0 - \sigma_{dr}\varepsilon_v(t)$$
$$= \gamma_0\left(1 - \frac{\varepsilon_v(t)}{\varepsilon_{vc}}\right)$$

We assume that the drawn material obeys the Maxwell equation, i.e., the rate of viscoelastic deformation is constant, due to the constancy of the stress σ_{dr} acting on the fibers. Then, the law of specific fracture energy evolution at a point M within the PZ can be rewritten as

$$\gamma(M, t) = \gamma_0\left[1 - \frac{t - t_*(M)}{t_r}\right] \tag{3.3}$$

where t is the present clock reading, $t_*(M)$ was the clock reading when the PZ tip passed through point M, and t_r is the time interval during which any fiber can withstand stress σ_{dr} (the elapsed time until fiber creep rupture). Creep lifetime t_r is considered to be a function of temperature T and the stress σ_{dr}. According to the fluctuation theory of fracture developed by Zhurkov et al.,[23] t_r is the exponential function

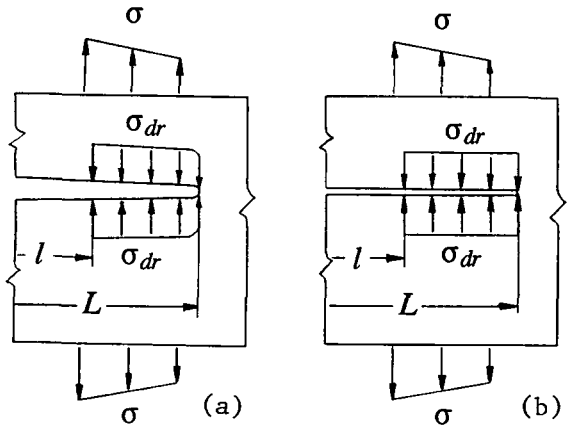

Figure 4 Boundary value problem for evaluation of COD and SIF: (a) plate with cut-out, (b) plate with slit.

$$t_r = t_0 \exp \frac{Q}{RT} \tag{3.4}$$

in which the stress-dependent activation energy Q is expressed as

$$Q = Q_0 - \chi \sigma_{dr} \tag{3.5}$$

In Eqs. (3.4) and (3.5), t_0 is a characteristic time, Q_0 is a constant part of the activation energy, and χ is the coefficient that reflects the material microstructure.

The driving force X_{PZ} for the PZ advance is given by the expression[15,18]

$$X_{PZ} = \frac{1}{E}(K_\infty + K_{dr})[K_\infty + (1 + 2\tilde{\gamma})K_{dr}] \tag{3.6}$$

or

$$X_{PZ} = 0 \tag{3.6'}$$

depending on whether the derivative of G with respect to L is positive or not. Above, K_∞ and K_{dr} designate the stress intensity factors (SIFs) at the CL tip due to remote stress σ and traction σ_{dr} acting along the PZ boundary (see Fig. 4). In Eq. (3.6),

$$E = E_0 \quad \text{or} \quad E = \frac{E_0}{1 - \nu^2}$$

for plane stress and plane strain, respectively; E_0 and ν are Young's modulus and Poisson's ratio of the original material.

If the driving forces equal zero, then the CL remains in a steady state, i.e.,

$$\frac{dl}{dt} = 0 \quad \frac{dL}{dt} = 0$$

The condition for a stationary PZ

$$X_{PZ} = 0$$

according to expression (3.6), results in two equations:

$$K_\infty + K_{dr} = 0 \quad K_\infty + (1 + 2\tilde{\gamma})K_{dr} = 0$$

Each of them leads to a stationary (equilibrium) size of the CL at a prescribed crack length l. The first gives the solution that coincides with the CL size in the Dugdale–Barenblatt (D–B) model and corresponds to an unstable state, while the second yields the solution L_{eq} (smaller than the length for the D–B model, if $\tilde{\gamma} > 0$) at which the PZ is in a stable state.[16]

Equations (3.1), the right-hand sides of which are expressed by (3.2)–(3.2') and (3.6)–(3.6'), together with law (3.3) of rupture energy evolution are strongly nonlinear. The results presented below are based on the numerical solution of these equations. The fourth-order Runge–Kutta method can be used. At the nth step of the numerical procedure, the singular boundary value problem of linear elasticity for the current CL configuration, l^n and L^n, and for the load shown in Figure 4, is solved. The solution results in current values of CODs δ_∞^n and δ_{dr}^n, and of SIFs K_∞^n and K_{dr}^n. The current value of the specific rupture energy γ_n, at the current crack tip l^n, is determined by Eq. (3.3). Then, the current values X_{CR}^n and X_{PZ}^n, of driving forces X_{CR} and X_{PZ}, are computed according to expressions (3.2) and (3.6), respectively. The next time step, Δt_{n+1}, is selected so that conditions $l^{n+1} \le L^{n+1} \le L_{eq}^{n+1}$ are satisfied, and the error for the step does not exceed the prescribed maximum allowable error. The numerical process is stopped, when even an infinitesimal time step results in a relatively very large (the same order of magnitude as the specimen width W) crack advance. This signals instability (or the end) of the slow CL growth. The elapsed time until instability is called the lifetime, or the time to failure, and denoted by t_f.

The above numerical solution displays two types of CL behavior, depending on the particular values of the physical and geometrical quantities employed in the CL kinetic model. The first type [Fig. 5(a)] is a smooth CL growth. It occurs when the driving force X_{CR} is positive during the entire process, i.e., $J_1 > \gamma(t)$ for any time t. The second type [Fig. 5(b)] is a discontinuous (stepwise) CL advance, which consists of a succession of alternating initiations and arrests of the crack and PZ. [Please be aware that the time scale for Fig. 5(a) is different from that for Fig. 5(b).] Growth of the crack, with tip at point x, is initiated when the condition $J_1 = 2\gamma(t_i)$, $t_i > t(x)$, is met. At the beginning of each time step

$$J_1 < 2\gamma_0 \tag{3.7}$$

In the process of CL evolution, the PZ size can be smaller than equilibrium (underdeveloped PZ) or equilibrium (developed PZ). For example, during the process depicted in Figure 5(a), the PZ lags behind its equilibrium size; while in the process shown in Figure 5(b) the PZ maintains the equilibrium size

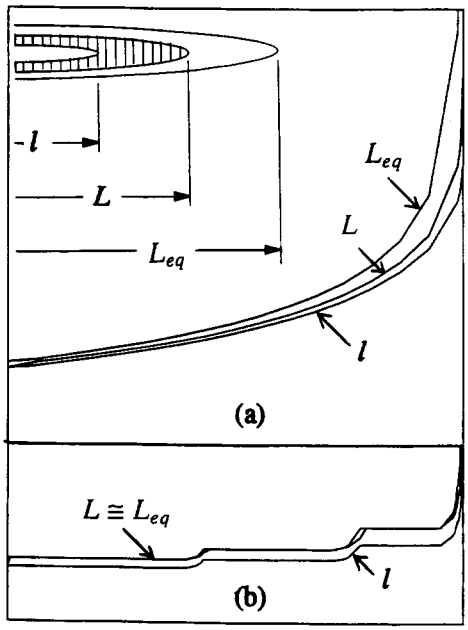

Figure 5 Two modes of crack layer growth: (a) smooth, (b) discontinuous (stepwise).

almost all of the time. The relationship between a current PZ size and its equilibrium size, depends mainly on the ratio of kinetic coefficients k_1 and k_2.

Analysis of the kinetic model shows that for all smooth processes, the lifetime t_f [see Fig. 5(a)] strongly depends on kinetic coefficients k_1 and k_2. However, the time to failure in the stepwise processes [see Fig. 5(b)] depends only weakly on these coefficients. For such processes, the rate of CL growth is mostly determined by how much smaller J_1 is than $2\gamma_0$, i.e., how much time precedes an increment of crack extension.

As numerous observations on PEs show, the quasi-brittle crack in PEs grows discontinuously under both constant and cyclic loadings.[12,13] For this reason, further modeling of the time–stress relationship is based on the corresponding behavior of the CL kinetic model. A higher level of remote stress σ, results in a more pronounced discontinuity of the slow crack growth. This means that the number of steps within the process decreases, and the size of each individual step increases, with increase of σ. This is illustrated in Figure 6, where two processes of slow crack growth under tension are shown. Figure 6(a) and (b) refer to relatively low and high applied stresses, respectively [note that the time scale for Fig. 6(a) is different from that for Fig. 6(b)]. These predictions of the model agree well with observations.[12]

4. TIME–STRESS–TEMPERATURE RELATION

A characteristic length scale l_* of the kinetic model is introduced as follows

$$l_* = \frac{2E\gamma_0}{\sigma_{dr}^2} \tag{4.1}$$

It is an important parameter that depends on properties of the original and drawn materials. Two other material characteristics introduced in the previous section, the drawing stress σ_{dr}, and the rupture time t_r of the drawn material, are used as scales of stresses and time, respectively. One more physical parameter of the kinetic model is the normalized drawing energy $\tilde{\gamma}$. The kinetic model explicitly accounts for the system geometry (sizes of the plate and initial length of the notch), as well as the loading conditions (simple or eccentric tension, pure or three-point bending, etc.). For simplicity, all further considerations in this study are confined to simple tension of a SEN specimen.

Let τ_f be the time to failure normalized by the rupture time t_r of the drawn material, $\bar{\sigma}$ be the applied stress normalized by the drawing stress σ_{dr}, and η stand for the specimen sizes (the notch length and plate width), each normalized by the characteristic length l_*:

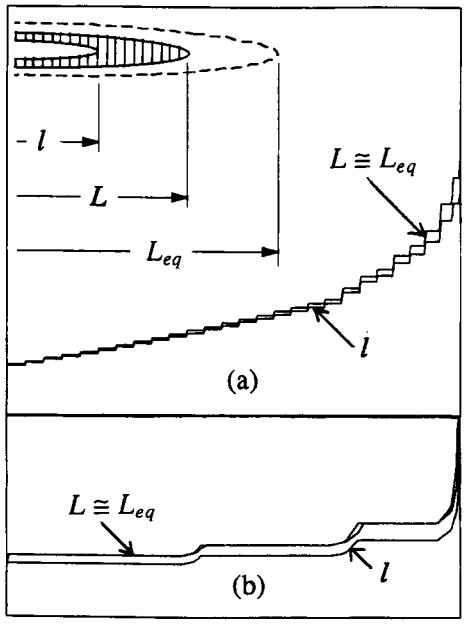

Figure 6 Stress dependence of discontinuous crack layer growth: (a) low stress ($\sigma = 0.25\ \sigma_{dr}$), (b) high stress ($\sigma = 0.75\ \sigma_{dr}$).

$$\tau_f = \frac{t_f}{t_r} \quad \bar{\sigma} = \frac{\sigma}{\sigma_{dr}} \quad \eta = \{\bar{l}_0, \bar{W}\}$$

If the material properties, specimen geometry, and applied stress are prescribed, a computer simulation of slow CL growth can be constructed by means of the numerical solution of Eq. (3.1). Analyzing the data of such numerical experiments, we obtain the following approximate relation between the lifetime and applied stress:

$$\log \tau_f = B - \beta \log \bar{\sigma} \tag{4.2}$$

The quantities B and β are in general functions of l_*, $\tilde{\gamma}$, and η. Numerical experiments with the kinetic model allows one to evaluate these functions. Specifically, our analysis shows that: (1) β weakly depends on $\tilde{\gamma}$ and can be considered to be a function of l_* and η only; (2) β varies between 2 and 5 for practical ranges of l_* and η; (3) B can be decomposed into the sum

$$B = B_1(l_*, \eta) + B_2(\tilde{\gamma})$$

i.e., for a given value of η (for given normalized sizes), curves B vs. l_* at various $\tilde{\gamma}$, are identical in shape to each other. As follows from comparison of the PZ sizes observed in PEs and predicted by the CL model,[17] the value of the normalized drawing energy $\tilde{\gamma}$, is close to one. All of the above means that the quantities B and β, as functions of the material parameters and specimen geometry, can be reduced to the form:

$$B = B(l_*, \eta) \quad \beta = \beta(l_*, \eta)$$

It is important to emphasize that both the theoretical and experimental relations, (4.2) and (2.1), respectively, establish a power dependence of lifetime t_f on applied stress σ; and the range of exponent β, from 2 to 5, predicted by the kinetic model, coincides with the range of exponent α observed for various kinds of PE.[2-6]

The characteristic length l_*, expressed by Eq. (4.1), is expected to be a function of temperature, since the material properties involved in this equation are temperature dependent. Therefore, quantities B and β are functions of temperature, as well. Temperature dependence of the material parameters in Eq. (4.1), as well as such dependence for the relaxation time t_r, can be found in experiments with unnotched specimens, i.e., independently of a slow crack growth observation. In the present study, the material parameters needed for the model are reconstructed from certain experimental data on crack growth, because of lack of data regarding the temperature dependence of the creep and rupture properties of the drawn material. First, the temperature dependence of exponent α for the particular material is determined. For example, the dependence can be found by a statistical analysis of the time–stress relationship at various temperatures reported for one of the PEs in Ref. 5. In this particular case, while the temperature increases from 42 to 80°C, exponent α increases from 3.0 to 4.8. In order to coordinate theoretical prediction with experimental observation, i.e., function $\beta(T)$ with function $\alpha(T)$, characteristic length l_* must be a certain decreasing function of temperature. This requirement results in a definite form of temperature dependence of material properties E, σ_{dr}, and γ_0. Since drawing stress σ_{dr}, and Young's modulus E, decrease with temperature almost proportionally to each other,[4] then it follows from expression (4.1) that fracture energy γ_0 must decrease faster with temperature than the drawing stress. For another PE examined in Ref. 6, exponent α is practically constant within the temperature range between 24 and 80°C. Hence, it follows for this case that length scale l_*, and as a result, ratio γ_0/σ_{dr}, are temperature independent. When the temperature dependence of the length scale l_* is established, the quantities B and β in Eq. (4.2) are readily determined as functions of temperature:

$$B = B(T, \eta) \quad \beta = \beta(T, \eta)$$

(the specimen geometry parameter η is prescribed).

Accounting for expressions (3.4) and (3.5), we reduce Eq. (4.2) to the following form:

$$t_f = t_0\left(\frac{\sigma}{\sigma_{dr}}\right)^{-\beta} \exp\left(\frac{Q_0 - \chi\sigma_{dr}}{RT} + b\right) \tag{4.3}$$

where $b = B/\log e$. According to the previous definitions, quantities b and β are the kinetic model parameters reflecting properties of the material and specimen geometry, while t_0, Q_0, and χ reflect the properties of the original and drawn materials only. Equation (4.3) is the time–stress–temperature relation resulting from the kinetic model of slow CL growth.

If for a certain material and specimen geometry, exponent α is temperature independent, then the kinetic model parameters B and β also do not depend on temperature. In this case the transition from one temperature to another, from T_1 to T_2, can be expressed in the form

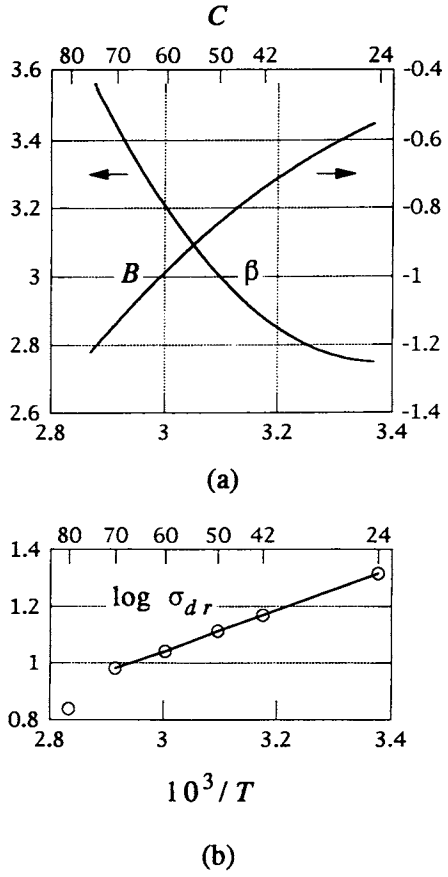

Figure 7 Temperature dependence: (a) crack layer parameters B and β, (b) drawing stress σ_{dr}.

$$\log t_f(T_2) = \log t_f(T_1) + 0.43\frac{Q_0}{R}\left(\frac{1}{T_2} - \frac{1}{T_1}\right) - 0.43\frac{\chi\sigma_{dr}}{R}\left(\frac{1}{T_2} - \frac{1}{T_1}\right) + \beta\log\left(\frac{\sigma_{dr}(T_2)}{\sigma_{dr}(T_1)}\right)$$

If the term with the activation energy Q_0 is considered as a horizontal shift (along the axis of log t_f), then the sum of the two following terms can be treated as a vertical shift (along the axis of log σ). This last equation represents the vertical shift in terms of material parameters σ_{dr} and χ. Remember that for the empirical methods discussed in Section 2, the vertical shift was a function of the indeterminate parameter σ_c.

Three material constants in Eq. (4.3) are left to be established: characteristic time t_0, activation energy Q_0, and coefficient χ. If activation energy Q_0 is taken as 100 kJ/mol (this value is reported as the average for PEs), then the other two parameters, t_0 and χ, can be determined from the data of experimental observations. The procedure for finding these parameters is described in Appendix C.

In order to test the predictive power of the kinetic model, we employ the most comprehensive experimental data, which is reported in Ref. 5. The experiments were conducted on SEN tensile specimens, each with size $l_0 = 3.5$ mm and $W = 10.0$ mm. The material is the ethylene–hexene copolymer with 4.5 butyl branches per 1000 C, M_n = 15,000, M_w = 170,000, and density = 0.938 g/cm^3. For this material, the yield stress σ_y, at room temperature (24°C) equals 21.5 MPa. Since the drawing stress σ_{dr} is not reported, we assume $\sigma_{dr} \approx \sigma_y$. The temperature dependence of σ_y is reported in Ref. 5, and the σ_{dr} temperature dependence follows that for σ_y.[24] The model parameters are selected so that the lifetime's stress dependence, obtained on the basis of Eq. (4.3), and measured experimentally, agree for temperatures 50 and 70°C (see Appendix C). This suggests the following temperature dependence of the characteristic length:

$$\log l_* = -4.17 + \frac{663}{T}$$

Corresponding functions B and β of temperature are shown in Figure 7(a), and the remaining constants are evaluated as

$$t_0 = 6.46 \times 10^{-12} \text{ min} \quad \chi = 0.63 \times 10^{-3} \text{ m}^3/\text{mol}$$

The temperature dependence of the drawing stress σ_{dr} (assumed equal to the dependence reported for σ_y in Ref. 5), is shown in Fig. 7(b).

The data of the direct measurements[4,5] (points) and the theoretical predictions of Eq. (4.3) (lines) are combined in Fig. 8. The dashed lines correspond to the adjustment temperatures 70 and 50°C. The

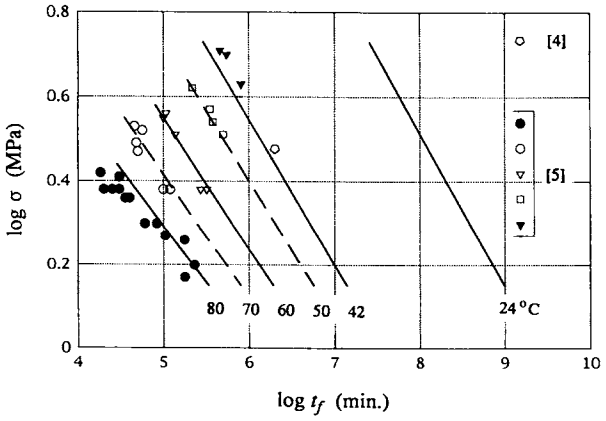

Figure 8 Experimental observations (points) and theoretical predictions (lines).

theoretical results agree with the experimental results (within scatter of the data), not only at 60°C (the temperature of interpolation) but also at 80 and 42°C (the temperatures of extrapolation). Experimental data for temperature 24°C does not exist. Evidently, the CL kinetic model correctly describes the stress lifetime relationships for brittle fracture at various temperatures. Simultaneously, the ranges of the model parameters B and β, and the qualities of their dependencies on characteristic length l_*, indicate the possibility of a good description for each PE investigated in Refs. 2–6.

Fig. 9 displays stress lifetime lines for room temperature (24°C) obtained by three different methods (see Appendix D). Line 1 results from the treatment proposed in Ref. 5. Line 2 was produced by the double shift Eqs. (2.4) and (2.5), acting on the 80°C data from Ref. 5. Line 3 was calculated by Eq. (4.3). Lines 1 and 3 are almost parallel, but the slope of line 2 is noticeably smaller because shifts (2.4) and (2.5) translate the slope of the 80°C line, to any other temperature. The predictions of the kinetic model and of method in Refs. 7 and 8 [Eqs. (2.4) and (2.5)] are similar, and forecast lifetimes somewhat longer than those reported in Ref. 5.

To conclude this section, note that in order to determine the lifetime prediction for a specimen of the same material, but with a different size, within the proposed framework it is only necessary to recalculate the values of the kinetic model characteristics B and β in Eq. (4.3). For example, if for the specified specimen, the notch depth l_0 decreases from 3.5 to 0.5 mm, then at room temperature (24°C) and within the applied stress range $(0.2\sigma_{dr} - 0.4\sigma_{dr})$, the lifetime becomes 18–12 times longer.

5. ACCELERATED TESTING FOR LIFETIME

As stated above, all the material characteristics required in the CL kinetic model can be determined from tests that do not involve slow crack growth. Two types of tests are needed for the material characterization. The first type are simple ramp tests, which provide Young's modulus E_0, Poisson's ratio ν, drawing stress σ_{dr}, natural draw ratio λ_n and drawing energy γ_{dr}, at various temperatures. The second type are creep tests of the drawn fibers under σ_{dr}. The characteristic time t_0, activation energy $Q = Q_0 - \chi\sigma_{dr}(T)$, and specific rupture energy $\gamma_0(T)$ should be extracted at various temperatures. Both test types can be performed on unnotched specimens.

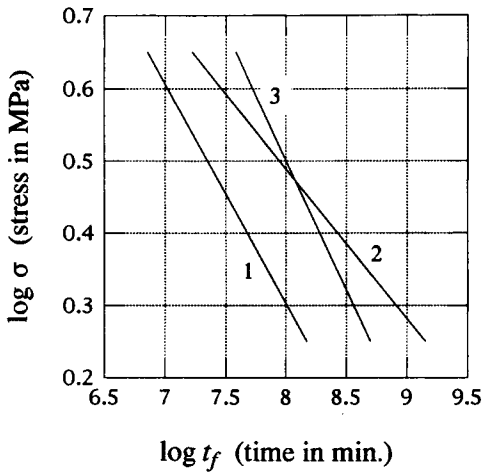

Figure 9 Predictions of lifetime at room temperature.

The determined temperature dependence of the material characteristics leads to the determination of the temperature dependence of the characteristic length l_* and rupture time t_r. Then, computer simulations of slow crack growth based on the CL kinetic model result in the determinations of parameters B and β in Eq. (4.3), as functions of temperature. Thus, all quantities in Eq. (4.3) are known, and predictions of lifetime can be computed for a range of temperatures.

6. SUMMARY

1. Brittle fracture, resulting from slow crack growth in PEs can be adequately modeled using the kinetic equations of CL growth. The CL kinetic model realistically describes the discontinuous (stepwise) process commonly observed in PEs.
2. At relatively low stresses, the CL kinetic model predicts a power dependence of the time to failure t_f on applied stress σ:

$$t_f \propto \sigma^{-\beta}$$

   where exponent β ranges from 2 to 5. This β range is coincident with that observed experimentally for PEs.
3. The connections between the lifetime stress relations at various temperatures are strongly associated with the temperature dependence of time to failure described by the fluctuation theory of fracture. According to the theory, the time to rupture of the drawn fibers, t_r, depends on temperature as

$$t_r = t_0 \exp \frac{Q_0 - \chi\sigma_{dr}(T)}{RT}$$

where t_0, Q_0, and χ are the parameters of the drawn material, σ_{dr} is the temperature dependent stress acting on the fibers, R is the universal gas constant, and T is the temperature in degrees Kelvin.

4. The time–stress–temperature correspondence resulting from the CL kinetic model, can be presented in the following form:

$$t_f = t_0 \left(\frac{\sigma}{\sigma_{dr}}\right)^{-\beta} \exp\left(\frac{Q_0 - \chi\sigma_{dr}}{RT} + b\right)$$

Parameters b and β are obtained from the numerical solution of the CL kinetic equations for the particular boundary value problem. Both parameters are usually, but not always temperature independent.

5. Lifetime prediction, within the framework of the proposed approach, is reduced to experimental measurements of the material properties, and computer simulations of slow crack growth using the determined material parameters, along with the other particular conditions such as temperature, specimen geometry, shape, and magnitude of prescribed loading.
6. The tests for evaluation of the material properties use smooth specimens, and require relatively short-term observations. Thus, the lifetime prediction method proposed in this study can be used as an accelerated test for the determination of PE performance.

7. CONCLUDING REMARK

The dependence of the kinetic model behavior on temperature mainly results from the temperature dependence of the time to rupture t_r of the drawn fibers. An increase in temperature causes a decrease in the rupture time. A reduction in rupture time can be achieved by the introduction of other agents, such as fatigue loading, chemical exposure, etc. These agents, in combination with slow crack growth modeling, provide the possibility for developing alternative accelerated tests for the brittle fracture of PEs.

APPENDIX A

According to Figure 7 of Ref. 6, at 80°C

$$\log t_f = 4.0 - 2.6 \log \sigma \qquad \text{(A.1)}$$

and at 24°C

$$\log t_f = 6.4 - 2.6 \log \sigma \qquad \text{(A.2)}$$

Here and after, time is measured in minutes and stress in MPa. Taking into account Eq. (A.1), the transition from 80 to 24°C by means of shifts (2.4) and (2.5) is expressed as

$$\log t_f = 4.0 + (0.109 + 2.6 \times 0.0116)\Delta T \log e - 2.6 \log \sigma$$

where $\Delta T = 56$ K. So, the shifts result in the following time–stress relation at 24°C:

$$\log t'_f = 7.4 - 2.6 \log \sigma \qquad \text{(A.3)}$$

Comparison of Eqs. (A.2) and (A.3) shows that method of Refs. 7 and 8 leads to the error

$$\log t'_f - \log t_f = 1.0$$

i.e., the prediction of the method is 10 times as big as direct measurements.

APPENDIX B

As follows from Figure 3 of Ref. 5, at 80°C

$$\log t_f = 6.4 - 4.8 \log \sigma \qquad \text{(B.1)}$$

and at 42°C

$$\log t_f = 7.9 - 3.0 \log \sigma \qquad \text{(B.2)}$$

Shifts (2.4) and (2.5) from 80 to 42°C result in the time–stress dependence:

$$\log t'_f = 9.2 - 4.8 \log \sigma \qquad \text{(B.3)}$$

If $\sigma = 5$ MPa, then the lifetime (B.2) measured directly in Ref. 5 and the lifetime (B.3) predicted on the basis of method in Refs. 7 and 8 practically coincide; but at lower stresses lifetime (B.3) can exceed lifetime (B.2) more than 10 times [e.g., at

σ = 1 MPa, lifetime (B.3) is 20 times as much as lifetime (B.2)].

APPENDIX C

The time–stress relation[5] can be approximated by (see Fig. 3 in Ref. 5)

$$\log t_f = 6.4 - 3.4 \log \sigma \qquad \text{(C.1)}$$

for 70°C, and by

$$\log t_f = 7.1 - 3.0 \log \sigma \qquad \text{(C.2)}$$

for 50°C. Our kinetic model provides a time–stress relation for the selected specimen geometry as follows:

$$\log t_f = \log t_0 + \frac{Q_0 - \chi\sigma_{dr}}{RT} \log e + B(l_*) - \beta(l_*)\log\left(\frac{\sigma}{\sigma_{dr}}\right) \qquad \text{(C.3)}$$

Let l_* be represented as the following function of temperature:

$$\log l_* = \omega_0 + \omega_1\left(\frac{10^3}{T}\right)\sigma$$

where ω_0 and ω_1 are unknown coefficients. These coefficients are selected so that the values of function β in Eq. (C.3) coincide with the values of the coefficients of log σ in Eqs. (C.1) and (C.2). According to the numerical solution of the kinetic model equations, β takes values 3.4 and 3.0, if log l_* is equal to −2.24 and −2.12, respectively. So, the first value of log l_* corresponds to $10^3/T$ = 2.915 (70°C), and the second value to $10^3/T$ = 3.096 (50°C). The system of two equations with respect to two unknowns yields

$$\omega_0 = -4.17 \quad \omega_1 = 0.663$$

Now B and β in Eq. (C.3) have been determined as functions of temperature. This means the time–stress relation (C.3) of the kinetic model contains three unknown constants t_0, Q_0, and χ, and the known functions of temperature [σ_{dr} (actually σ_y) is reported as a function of temperature in Ref. 5]. If one accepts

$$Q_0 = 100 \text{ kJ/mol}$$

and requires lifetimes (C.3) at 70 and 50°C to equal lifetimes (C.1) and (C.2), respectively, then the remaining two constants will be

$$t_0 = 6.46 \times 10^{-12} \text{ min} \quad \chi = 0.63 \times 10^{-3} \text{ m}^3/\text{mol}$$

Note that if coefficient α in Eq. (2.1) for the particular material does not depend on T, then l_* is determined by the condition

$$\beta(l_*) = \alpha$$

B and β are taken as constants, and the procedure for finding t_0 and χ remains the same.

APPENDIX D

The time–stress relation at 24°C resulting from the data reported in Ref. 5 can be written as:

$$\log t_f = 9.0 - 3.3 \log \sigma$$

Let shifts (2.4) and (2.5) be employed to obtain the time–stress relation for 24°C, from equation (B.1) for 80°C. Then,

$$\log t_f = 6.4 + (0.109 + 4.8 \times 0.0116)\Delta T \log e - 4.8 \log \sigma$$

where ΔT = 56 K; or

$$\log t_f = 10.4 - 4.8 \log \sigma$$

With the constants and functions determined in Appendix C, Eq. (C.3) establishes the following time–stress relation for 24°C:

$$\log t_f = 9.4 - 2.8 \log \sigma$$

This is the lifetime prediction based on the CL kinetic model.

REFERENCES

1. J. G. Williams, *Fracture Mechanics of Polymers*, Halsted Press, New York, 1987.
2. X. Lu and N. Brown, *J. Polym. Sci.*, **21**, 2217 (1986).
3. X. Lu and N. Brown, *J. Polym. Sci.*, **21**, 4081 (1986).

4. Y. L. Huang and N. Brown, *J. Polym. Sci., Part B: Phys.*, **28,** 2007 (1990).
5. X. Lu and N. Brown, *J. Mater. Sci.*, **25,** 29 (1990).
6. X. Lu and N. Brown, *J. Mater. Sci.*, **26,** 612 (1991).
7. C. F. Popelar, C. H. Popelar, and V. H. Kenner, *Polym. Eng. Sci.*, **30,** 577 (1990).
8. C. H. Popelar, V. H. Kenner, and J. P. Wooster, *Polym. Eng. Sci.*, **31,** 1693 (1991).
9. T. L. Carte, M. Klein, and A. Moet, *Soc. Plastic Eng. Ann. Tech. Conf.*, **3,** 3228 (1994).
10. B. V. Kostrov, L. V. Nikitin, and L. M. Flitman, *Izv. AN SSSR, Mekhanica Tverdogo Tela*, **4**(3), 105 (1969).
11. R. A. Schapery, *Inter. J. Fracture*, **11,** 141, 369, 549 (1975).
12. X. Lu, R. Qian, and N. Brown, *J. Mater. Sci.*, **26,** 917 (1991).
13. R. W. Hertzberg and J. A. Manson, *Fatigue of Engineering Plastics*, Academic Press, New York, 1980.
14. A. Chudnovsky, V. Dunaevsky, and V. Khandogin, *Arch. Mech.*, **30,** 165 (1978).
15. K. Kadota and A. Chudnovsky, *Proc. ASME Meeting*, 101 (1991).
16. A. Stojimirovic and A. Chudnovsky, *Inter. J. Fracture*, **57,** 281 (1992).
17. A. Stojimirovic, K. Kadota, and A. Chudnovsky, *J. Appl. Polym. Sci.*, **46,** 1051 (1992).
18. K. Kadota and A. Chudnovsky, *Polym. Eng. Sci.*, **32,** 1097 (1992).
19. A. Chudnovsky and K. Kadota, *Proc. PACAM III*, 419 (1993).
20. K. Kadota, S. Chum, and A. Chudnovsky, *J. Appl. Polym. Sci.*, **49,** 863 (1993).
21. X. Wang, N. Brown, and L. Frager, *Polymer*, **30,** 453 (1989).
22. X. Wang and N. Brown, *Polymer*, **30,** 1457 (1989).
23. S. N. Zhurkov, *Inter. J. Fract. Mechanics*, **1,** 311 (1965).
24. A. Chudnovsky, A. Kim, T.-J. Chen, K. Sehanobish, and C. P. Bosnyak, *ASME Winter Annual Meeting*, to appear.

Received October 20, 1994
Accepted December 31, 1994